## General Disclaimer

## One or more of the Following Statements may affect this Document

- This document has been reproduced from the best copy furnished by the organizational source. It is being released in the interest of making available as much information as possible.

- This document may contain data, which exceeds the sheet parameters. It was furnished in this condition by the organizational source and is the best copy available.

- This document may contain tone-on-tone or color graphs, charts and/or pictures, which have been reproduced in black and white.

- This document is paginated as submitted by the original source.

- Portions of this document are not fully legible due to the historical nature of some of the material. However, it is the best reproduction available from the original submission.

NASA TECHNICAL MEMORANDUM

NASA TM X- 73,206

NASA TM X 73,206

# BAND STRUCTURE OF W AND Mo BY EMPIRICAL PSEUDOPOTENTIAL METHOD

C. Guha Sridhar and Ellis E. Whiting

Ames Research Center
Moffett Field, California 94035


February 1977

| 1. Report No. NASA TM X-73,206 | 2. Government Accession No. | 3. Recipient's Catalog No. |
|---|---|---|
| 4. Title and Subtitle<br>BAND STRUCTURE OF W AND Mo BY EMPIRICAL PSEUDOPOTENTIAL METHOD | | 5. Report Date<br>6. Performing Organization Code |
| 7. Author(s)<br>C. Guha Sridhar* and Ellis E. Whiting | | 8. Performing Organization Report No.<br>A-6915 |
| 9. Performing Organization Name and Address<br>Ames Research Center<br>Moffett Field, California 94035 | | 10. Work Unit No.<br>506-16-12<br>11. Contract or Grant No. |
| 12. Sponsoring Agency Name and Address<br>National Aeronautics and Space Administration<br>Washington, D. C. 20546 | | 13. Type of Report and Period Covered<br>Technical Memorandum<br>14. Sponsoring Agency Code |

15. Supplementary Notes

*Contractor

16. Abstract

The empirical pseudopotential method (EPM) is used to calculate the band structure of tungsten and molybdenum. Agreement between the calculated reflectivity, density of states, density of states at the Fermi surface and location of the Fermi surface from this study and experimental measurements and previous calculations is good. Also the charge distribution shows the proper topological distribution of charge for a bcc crystal.

| 17. Key Words (Suggested by Author(s)) | 18. Distribution Statement |
|---|---|
| Band structure of tungsten and molybdenum<br>Optical properties<br>Fermi surface | Unlimited<br>STAR Category - 76 |

| 19. Security Classif. (of this report) | 20. Security Classif. (of this page) | 21. No. of Pages | 22. Price* |
|---|---|---|---|
| Unclassified | Unclassified | 28 | $3.75 |

*For sale by the National Technical Information Service, Springfield, Virginia 22161

# BAND STRUCTURE OF W AND Mo BY THE EMPIRICAL PSEUDOPOTENTIAL METHOD

C. Guha Sridhar* and Ellis E. Whiting

Ames Research Center

## INTRODUCTION

The purpose of this paper is to present a calculation of the band structure of W and Mo by the empirical pseudopotential method (EPM). Both of these elements are in group VI of the periodic table, are transition metals, have a body centered cubic crystal structure and have interesting catalytic and superconducting properties. The availability of reliable band structures of these transition metals would be very helpful in understanding, theoretically, many of their physical and chemical properties and to help predict the properties of suitably chosen alloys.

The calculations of the band structure of W and Mo made previous to the present study are summarized in the next section. Although these calculations have been very valuable, there is some question about the accuracy of the approximation used and it is always helpful to have other independent calculations for comparison.

Recently, the optical reflectivity of both W and Mo was measured by Weaver, Lynch and Olson (refs. 1 and 2) over a wide frequency range. The availability of these data made it possible for us to undertake a new and independent calculation of band structure of W and Mo by using the empirical pseudopotential method.

A complete description of the EPM is given in reference 3 and a few appropriate comments are presented in the Method section. However, as a means of introduction, in the EPM the crystal potential is approximated by an expression containing several adjustable parameters, called form factors. An approximate set of form factors are chosen to initiate an iterative procedure. A band structure is calculated using these form factors and then the band structure is used to calculate those properties that are to be used to indicate empirical adjustments to the form factors. After the form factors are adjusted, to provide better agreement with the chosen properties, the process is repeated until the calculated properties are believed to be adequate.

In the present study, the form factors were adjusted by comparing the calculated reflectivity spectrum with the data (refs. 1 and 2) mentioned above and the location of the calculated Fermi surface (refs. 4 and 5), and results are also given in references 6 and 7 for W and reference 8 for Mo. In addition, the calculated charge density in the (110) plane was plotted

*Contractor.

and used to indicate adjustments to the form factors to give a reasonable qualitative appearance to the charge distribution to obtain a stable crystal.

## PREVIOUS CALCULATIONS

*W-* The first band structure calculation for tungsten was done by Manning and Chodorow (ref. 9), using a cellular method. Later Loucks (ref. 10) (for the Cr group metals) and Matthiess (ref. 4) (for W) independently calculated the band structure and Fermi surface by using the nonrelativistic augmented plane wave (APW) method. More recently Petroff and Viswanathan (ref. 11) calculated the band structure and photoemission spectrum of tungsten by the APW method. Also, Lomer (ref. 5) has proposed a model Fermi surface for the chromium group metals based on Woods APW calculation on iron (ref. 12).

Matthiess (ref. 13) has adjusted his band structure by introducing the spin orbit coupling to fit the Fermi surface data. Loucks (ref. 14) later modified his band structure calculation by introducing relativistic corrections in the APW calculation and then calculated the Fermi surface. More recently, band calculations by the Relativistic Augmented Plane Wave (RAPW) method and experimental volume and surface photoemission spectra have been published by Christensen and Feuerbacher (ref. 15).

*Mo-* The band structure and Fermi surface of Mo were calculated by Loucks (ref. 10). Petroff and Viswanathan (ref. 11) have calculated the band structure and density of states. Recently Iverson and Hodges (ref. 16) derived nonrelativistic energy bands by the renormalized atom method and determined the Fermi surface using an interpolated band structure. They also used the de-Haas-van-Alphen data for the neck of the electron "jack" and the electron "lens" to derive the spin orbit parameter.

The density of states was calculated by Geguzin et al. (ref. 17) by using the Green's function method. Pickett and Allen (ref. 18) used the Slater Koster interpolation scheme on the APW band calculation of reference 11 to find the density of states. Koelling et al. (refs. 19 and 20) have calculated the optical properties, the Fermi surface and the density of states.

## METHOD

The diagonalization of large secular determinants in the pseudopotential calculations involves large amounts of computer time. Thus, an efficient iterative method for searching for an empirical pseudopotential which provides a near optimum agreement with experimental data is important. In the past, an inspection method (ref. 3) and nonlinear optimization schemes have been used. These schemes had great success in the calculation of band structures where single k-points in the Brillouin zone play a dominant role in determining the optical properties. However, there are many elements which display

very strong "volume" effects where the main peaks in the reflectivity spectrum arise not from "critical points" but from large regions throughout the Brillouin zone. Any attempt to label a given peak in the reflectivity spectrum by assigning a single energy separation at a single k-point would, thus, be useless. To account for this volume effect, we have developed a new efficient iterative technique for finding the near optimum pseudopotential. The details of this method have been described in reference 22. The five pseudopotential parameters for W and Mo are given in table 1.

## RESULTS

### Band Structure

Figures 1(a) and 1(b) show the band structures of W and Mo. Since these band structures are very similar, they will be discussed together. There are several striking differences between the APW calculations (refs. 4 and 11) and the present calculation.

(i) $\Delta$: Near its end points close to $\Gamma$, the present $\Delta_1$ band lies above the $\Delta_2$ band, but dips below this band at a point halfway between the $\Gamma$ and H symmetry points. No dip is observed in the work of Matthiess (ref. 4) and Petroff and Viswanathan (ref. 11), in which the $\Delta_1$ band has a free electronlike shape and lies well above the $\Delta_2$ and $\Delta_5$ bands.

(ii) $\Sigma$: The $N_4$ state is low compared to the APW (refs. 4 and 11) results. As a consequence, for W the $\Sigma_4$ band crosses the $\Sigma_1$ band. In addition, for both W and Mo the present $\Sigma_4$ band is relatively parallel to the $\Sigma_2$ band over most of the plot. Thus, even though the dipole matrix elements for this band pair are small, the effect on the calculated reflectivity spectrum will be significant because of the large joint density of states associated with this parallel band pair.

(iii) The present band ordering at the H symmetry point is somewhat unusual. That is, $H_1$ lies below $H_{15}$, while one expects the $H_1$ (7S) state to be higher in energy than $H_{15}$ (6p). The expected ordering is found in references 4 and 11. In EPM calculations, the higher level (>5 eV) energy states are inherently less accurate than the lower energy states because of the truncation of the form factors at lower wave numbers. The assumed correct ordering might be achieved by using a nonlocal p-potential. However, we have avoided any such alteration of the pseudopotential because the main intent of the present work is to provide an accurate description of the bands lying within about 5 eV of the Fermi level, and also to keep the number of adjustable parameters to a minimum.

(iv) In the case of Mo, the $P_1$ and $P_3$ states are reversed in comparison to W. Also, the separation $P_1 - P_3$ is larger for Mo than for W. In the APW calculation (refs. 4 and 11), the $P_1$ state lies above the $P_3$ state.

(v) Table 2 shows the comparison of some band separations. For W, the s-d separation is larger than the previous calculation (ref. 4) and the occupied d-bandwidth is less than the previous calculation. The s-p and d-bandwidths seem to be in reasonable agreement with the previous results.

(vi) In the present calculations, $\Gamma_{25'} - \Gamma_1$ for Mo has a value that is the average of the values found in the two previous calculations (refs. 11 and 16). However, $H_{25'} - \Gamma_1$ has a higher value compared to both earlier calculations. The value of the d-bandwidth and occupied d-bandwidth from the present calculations both have smaller values than the earlier results (refs. 11 and 16). The occupied d-bandwidth ($E_F - H_{12}$) is especially very much smaller than the previous results. On the other hand, the present occupied s-d bandwidth ($E_F - \Gamma_1$) is larger than the two earlier results. The origin of the differences mentioned above could be due to a stronger s-d hybridization effect in the EPM, and the truncation of the local pseudopotential, which would cause the higher s-p bands to be too low.

## Density of States

The calculated density of states, N(E) is given in figures 2(a) and (b) for W and Mo, respectively. The histograms are calculated with 0.1 eV resolution. The cutoff point is the Fermi energy and the estimated uncertainty of its position is about 0.05 eV. For W, the theoretical result is superimposed on the experiment of Zeisse (ref. 23). Table 3 lists the peak locations of the density of states for the present calculation and for previous calculations and experiments.

For W, the agreement of the density of occupied energy states is good to within about 0.3 eV with both previous APW calculations (refs. 4 and 11). The density of states at the Fermi level $N(E_F)$ is 0.3 states of one spin/eV atom and is in good agreement with the APW calculations. However, McMillan (ref. 24) obtained a value of 0.15 states of one spin/eV-atom from experimental values of the superconducting transition temperature and the electronic specific heat by using a strong coupling formulation. The agreement with McMillan's result is poor.

For Mo, the two experimental photoemission measurements show DOS peaks below the Fermi level of -0.5, -1.6, -3.9 eV from reference 25 and of -1.5 and -3.7 eV from reference 26. Geguzin et al. (ref. 17) calculated DOS by using the Green's function method and found peaks at -1.5, -2.7, -3.0, -3.8 and -4.2 eV. Petroff and Viswanathan (ref. 11) calculated the same peaks by the APW method. In the present calculation, peaks are found at -0.5, -1.5, -2.5, -3.15 and -4.1 eV. It is clear that none of the calculations or the measurements gives completely consistent results. Thus, it is diffitult to conclude whether our result is more or less accurate than the others. However, the results of the density of states at the Fermi level agree very well. McMillan's (ref. 24) strong coupling formulation gives 0.28 states of one spin/eV-atom, as does Pickett and Allen (ref. 18), Petroff and Viswanathan (ref. 11), and the present study, whereas Geguzin et al. (ref. 17) finds a value of 0.31 spin/eV-atom.

## Reflectivity

In this subsection and the next two, we show the final iterated values of the calculated properties that were used to adjust the form factors. The good agreement between the final calculated and experimental results indicates that the resultant band structure discussed above is reasonably accurate.

The calculated and experimental spectra are shown in figures 3 and 4. There are two theoretical curves on each figure, one for the nondirect transition method. The iteration scheme used only the spectrum given by the direct transition model to adjust the form factors. After convergence, the curve for the nondirect transition method was calculated using the same form factors. The direct transition model predicts a spectrum which has a reflectivity approximately 10% higher than the data. Although this agreement is considered very good, the difference may be in part due to the relative inaccuracies involved in using the pseudo wavefunction to calculate the dipole transition matrix elements. The nondirect model assumes the nonconservation of crystal momentum $\vec{k}$. Both curves are shown because there has been significant discussion of both in the literature (refs. 27-29).

Clearly the calculated reflectivity by the direct transition method is in quite good agreement for W up to 4.5 eV and for Mo up to 3.5 eV. Further work to improve the calculation at higher energy levels could be done, but the present results appear adequate for our purposes.

## Fermi Surface

The central cross sections for the Fermi surfaces of W and Mo are shown in figures 5 and 6. The calculated Fermi energy contours are shown as the solid curves.

For W, the experimental data (broken contours) are taken from Walsh and Grimes (ref. 6) and from Sparlin (ref. 7). The data of Walsh and Grimes give the linear dimensions of that portion of the electron "jack" and the hole octahedron in the (110) plane and the data of Sparlin give the hole ellipsoids at symmetry point N. Sparlin's data were taken from his de-Haas-van-Alphen results. The agreement between the measured and calculated Fermi surface dimensions in the (110) plane is fairly good. The fact that the electron "jack" and the hole "octahedron" fail to touch along $\Delta$ in experiment is readily explained in terms of the spin orbit coupling. This separation in W is estimated to be 5% of $\Gamma H$ distance. Matthiess and Watson (ref. 13) have estimated the 5d spin orbit coupling parameter in metallic W to be approximately 0.4 eV. Spin orbit coupling also causes the "lenses" inside the "necks" to reduce in size and perhaps disappear entirely.

The dimension of the hole ellipsoids at N is determined by the energy difference between $E(N_1')$ and the Fermi energy. Since $N_1'$ is primarily a 6-p state, this energy difference depends on the energy separation between the s-p and d bands.

The general features of the calculated Fermi surface of Mo are shown in figure 6 to be very similar to that obtained by Boiko et al. (ref. 8). The Fermi surface result agrees very well with Lomer's calculation (ref. 5) which is not shown in the figure.

The size of the Fermi surface obtained experimentally by Boiko et al. (ref. 8), where in experiment the relativistic effect is naturally included, was smaller for W than for Mo. They also observed the vanishing of the electron lens in W. As far as the present calculation is concerned, the Fermi surface dimensions of W are not significantly less than those for Mo. Precise values of the areas of Fermi surface have not been calculated because of the relative crudeness of the present interpolation scheme and because the calculation would involve the comparatively inaccurate method of adding up the grid squares.

## Charge Distribution

The charge distribution was calculated on a mesh using 70 points in 1/48 of the Brillouin zone. The charge density for each valence band can be written as

$$\rho_n(\bar{r}) = \int d^3k \sum_{\{P_R\}} |\psi_{n\bar{k}}(P_R\bar{r})|^2$$

where $\psi_{n\bar{k}}(\bar{r})$ is the wavefunction for the nth band at $\bar{k}$ and $\{P_R\}$ is the symmetry operator needed to generate selected wavefunctions. The charge distribution of a completely filled band is normalized to two electrons/band in the primitive cells. The total valence band charge density is the sum over $\rho_n$ of the completely and partially occupied bands.

Figures 7 through 10 show the individual valence bands and the sum of the valance bands charge densities. These charge densities are plotted on the (110) plane of the crystal.

In each case, figure (a) is for W and figure (b) is for Mo. Since there are no experimental charge distribution results available for transition metals, we will discuss the results of the two metals comparatively.

In figure 7(a) for the first valence band of W, we observe some nonspherical features and lobes, whereas in figure 7(b) for Mo a nearly spherical symmetry of the charge distribution is seen at the atoms. This is because in Mo, the s-d separation ($\Gamma_1 - H_{12}$) in the lowest lying state is 3.3 eV, whereas in W it is only 1.9 eV. Since in W the d-like state $H_{12}$ lies quite close to the s-like state, $\Gamma_1$, there is some hybridization which produces the lobes on the sides of the central atom.

In the second valence band of W (fig. 8(a)) we do not observe any long lobes on the two sides of the central atom, as observed in Mo (fig. 8(b)), but instead we see small lobes along the body diagonal that indicates the contribution of d-like states. The two long lobes on the sides of the central

contribution of d-like states. The two long lobes on the sides of the central atom arise from the $P_4$ state of xy symmetry.

The third valence band (figs. 9(a) and (b)) shows fairly strong maxima along the diagonal, which indicate major contributions from the d-states. The 4th and 5th valence bands are mostly empty below the Fermi level, and their charge distributions are not shown.

The total charge distribution of the occupied states is shown in figures 10(a) and 10(b). The maximum of the contours associated with each atom occurs near 1/4th of the interatomic distance. These are made up primarily from the lobes of the d-states. In the case of W, the lobes are considerably smaller than those in Mo, although the magnitude of the contours is comparable. This difference may be due to the fact that $(P_4 - H_{12})$ is only 1.0 eV in Mo and 2.25 eV in W.

## SUMMARY

An effective new scheme to determine the empirical pseudopotential has been used to calculate the band structures of W and Mo. The band structures for the two metals are similar, as expected, and both differ in several significant ways from previous APW calculations.

The present occupied density of states in W agrees very well with the previous APW calculations and experiment. The agreement in the case of Mo is fair with other experiments and theory. However, it is difficult to resolve the density of state peaks from photoemission measurements. Hence, the poor agreement, in the case of Mo with experiment, is not considered to be serious. The density of states at the Fermi surface shows excellent agreement with previous APW (refs. 4 and 11) calculations in the case of W. However, a reason for the poor agreement with McMillan's result (ref. 24) is unknown. In the case of Mo, this result shows good agreement with all the previous calculations (refs. 11, 17, 18, and 24).

The reflectivity of W and Mo has been calculated from 0-4.5 eV. The results look very good except for the region above 3.5 eV for Mo. The EPM iteration used the reflectivity spectrum calculated by the direct transition method to adjust the form factors. After the form factors were found in this way, a second reflectivity spectrum was also calculated using the nondirect transition method. The results from the two methods show some differences.

The cross sections of the Fermi surfaces for W and Mo have been mapped out. They show close agreement with an available data. W shows good agreement with Matthiess result and Mo shows good agreement with the original Lomers (ref. 5) model Fermi surface. The charge density was calculated for the (110) plane and show a qualitatively correct charge distribution. We believe that the present band calculations of W and Mo are sufficiently accurate to be used to calculate phonon coupling constants and bonding properties in alloys of these transition metals.

## REFERENCES


1. Weaver, J. H., Olson, C. G., and Lynch, D. W., Phys. Rev. B12, 1293 (1975).

2. Weaver, J. H., Lynch, D. W., and Olson, C. G., Phys. Rev. B10, 501 (1974).

3. Cohen, M. L. and Heine, V., Solid State Physics, edited by F. Seitz and D. Turnbull (Academic Press, New York) 1970, vol. 24.

4. Matthiess, L. F., Phys. Rev. 139, A 1893 (1965).

5. Lomer, W. M., Proc. Phys. Soc. (London), 84, 327 (1964).

6. Walsh, W. M., Jr., and Grimes, C. C., Phys. Rev. Lett., 13, 523 (1964).

7. Sparlin, D. M., Thesis, Northwestern Univ., 1964.

8. Boiko, V. V., Gasparov, V. A., and Gverdtsiteli, I. G., Sov. Phys. - JETP, 29, 267 (1967); Boiko, V. V. and Gasparov, V. A., ibid. 61, 1976 (1971); ibid. 34, 1054 (1972).

9. Manning, M. F. and Chodorow, M. I., Phys. Rev. 56, 787 (1939).

10. Loucks, T. L., Phys. Rev. 139, A1333 (1965).

11. Petroff, I. and Viswanathan, C. R., Phys. Rev. B4, 799 (1971).

12. Wood, J. H., Phys. Rev. 126, 517 (1962).

13. Matthiess, L. F. and Watson, R. E., Phys. Rev. Lett., 13, 526 (1964).

14. Loucks, T. L., Phys. Rev. 143, 506 (1966).

15. Christensen, N. E. and Feuerbacher, F., Phys. Rev. B10, 2349 (1974).

16. Iverson, R. J. and Hodges, L., Phys. Rev. B8, 1429 (1973).

17. Geguzin, I. I., Nikiforov, I. Ya., and Alperovich, G. I., Sov. Phys., Solid State, 15, 646 (1973).

18. Pickett, W. E. and Allen, P. B., Phys. Lett., 48A, 91 (1974).

19. Koelling, D. D., Mueller, F. M., and Veal, B. W., Phys. Rev. B10, 1290 (1974).

20. Koelling, D. D., Mueller, F. M., Arko, A. J., and Ketterson, J. B., Phys. Rev. B10, 4889 (1974).

21. Walter, John P. and Cohen, M. L., Phys. Rev. 183, 763 (1969).

22. Alward, J. F., Perlov, C. M., Fong, C. Y., and Sridhar, C. G., to be published in Phys. Rev. B.

23. Zeisse, C. R., Nat. Bur. Stand. Publ. Class T, Issue 323, 199 (1971).

24. McMillan, W. L., Phys. Rev. 167, 331 (1968).

25. Kress, K. A. and Lapeyre, G. J., Mat. Res. Symp., Nat. Bur. Stand., Nov. 1969.

26. Eastman, D. E., Solid State Commun., 7, 1697 (1969).

27. Berglund, C. N. and Spicer, W. E., Phys. Rev. 136, A1030 (1964).

28. Krolikowski, W. F. and Spicer, W. E., Phys. Rev. B1, 478 (1970).

29. Smith, N. V. and Spicer, W. E., Optics Commun. 1, 157 (1969).

TABLE 1.- EPM PARAMETERS[a]

| Parameter | Present results, Ry | |
|---|---|---|
| | Tungsten | Molybdenum |
| V(2) | -0.050 | -0.082 |
| V(4) | .035 | .101 |
| V(6) | .015 | .048 |
| V(8) | .109 | .069 |
| Depth of d-well | -3.96 | -3.90 |
| Width of d-well | | 1.09 Å |

[a]The argument of the form factors is given in units of $(2\pi/a)^2$ where a = 3.16 Å for W and a = 3.15 Å for Mo. The value of the free-electron parameter is $\gamma = 0.22\times10^{-49}$ g-cm$^3$ for W and $0.320\times10^{-49}$ for g-cm$^3$ for Mo.

TABLE 2.- INTERESTING BAND DIFFERENCES

| | s-d separation, eV | | d bandwidth, eV | Occupied d-bandwidth, eV | Occupied s-d bandwidth, eV | s-p bandwidth, eV |
|---|---|---|---|---|---|---|
| | $\Gamma_{25'} - \Gamma_1$ | $H_{25'} - \Gamma_1$ | $H_{25'} - H_{12}$ | $E_F - H_{12}$ | $E_F - \Gamma_1$ | $N_1' - \Gamma_1$ |
| Tungsten | | | | | | |
| Present result | 6.10 | 12.26 | 10.17 | 5.21 | 7.29 | 8.05 |
| Matthiess[4] | 5.51 | 11.26 | 10.51 | 6.17 | 6.92 | 8.63 |
| Petroff & Viswanathan[11] | 5.51 | 11.24 | 10.49 | 6.01 | 6.76 | 8.84 |
| Molybdenum | | | | | | |
| Present result | 5.06 | 11.99 | 8.73 | 3.83 | 7.09 | 8.30 |
| Petroff & Viswanathan[11] | 5.54 | 10.65 | 9.35 | 5.48 | 6.63 | 8.29 |
| Iverson & Hodges[16] | 4.42 | 10.07 | 10.40 | 6.24 | 5.92 | 8.33 |

TABLE 3.- COMPARISON OF DENSITY OF STATES

| | DOS peaks, eV | | | | | | DOS at FS states of one spin/eV atom |
|---|---|---|---|---|---|---|---|
| Tungsten | | | | | | | |
| Matthiess (APW)[4] | -1.6 | -3.0 | -4.0 | | | | 0.28 |
| Petroff & Viswanathan (APW)[11] | -1.5 | -3.2 | -4.18 | | | | .28 |
| Present | -1.8 | -3.0 | -4.15 | | | | .30 |
| Molybdenum | | | | | | | |
| Kress & Lapeyre[25] | -.5 | -1.6 | | | -3.9 | | |
| Eastman[26] | | -1.5 | | | -3.7 | | |
| Petroff & Viswanathan[11] | | -1.3 | -2.72 | | -3.7 | -4.1 | .28 |
| Geguzin et al.[17] | | -1.5 | -2.7 | -3.0 | -3.8 | -4.2 | .31 |
| Present | .5 | -1.5 | -2.5 | -3.15 | | -4.1 | .28 |

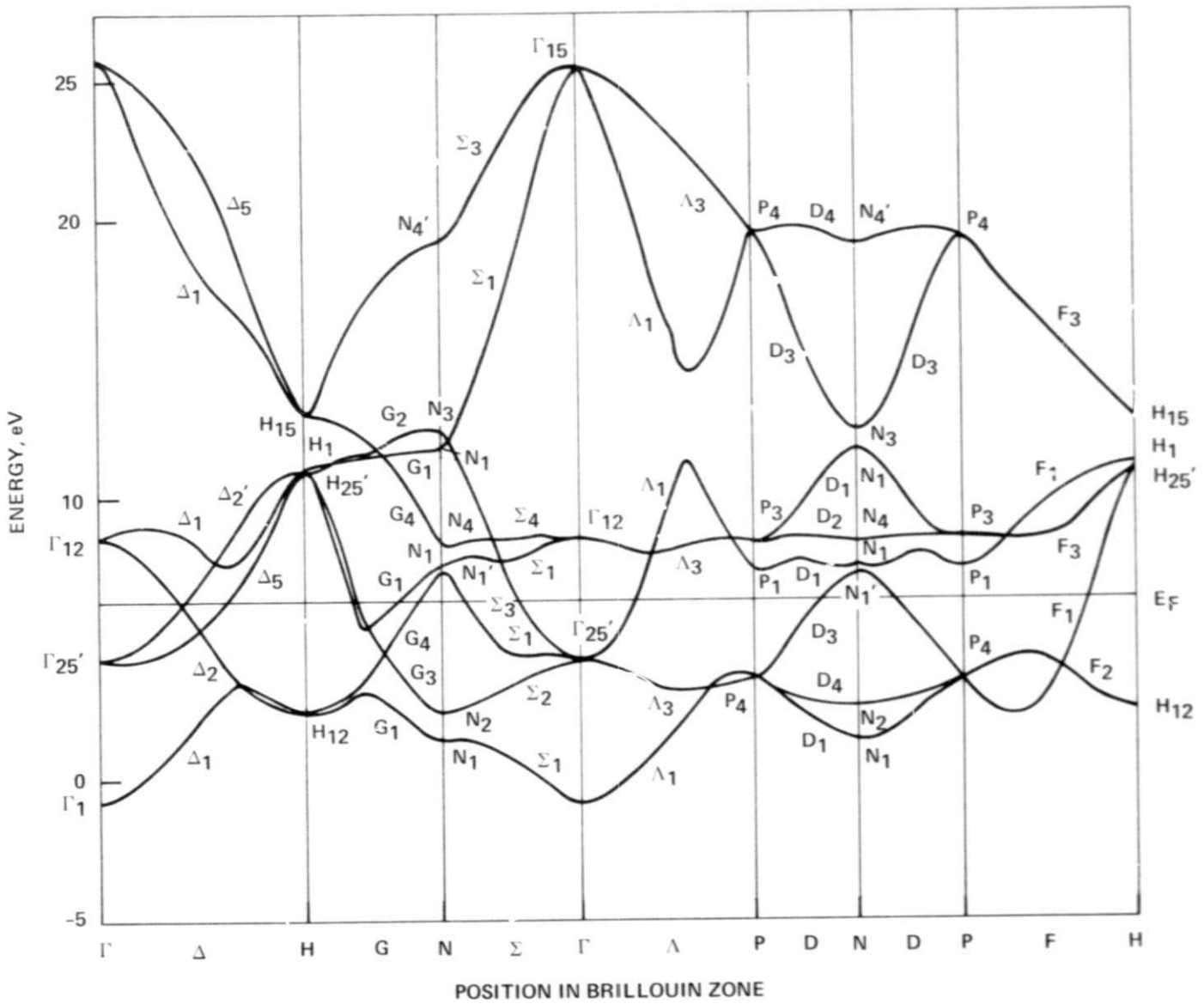


(a) W

Figure 1.- Band structure.

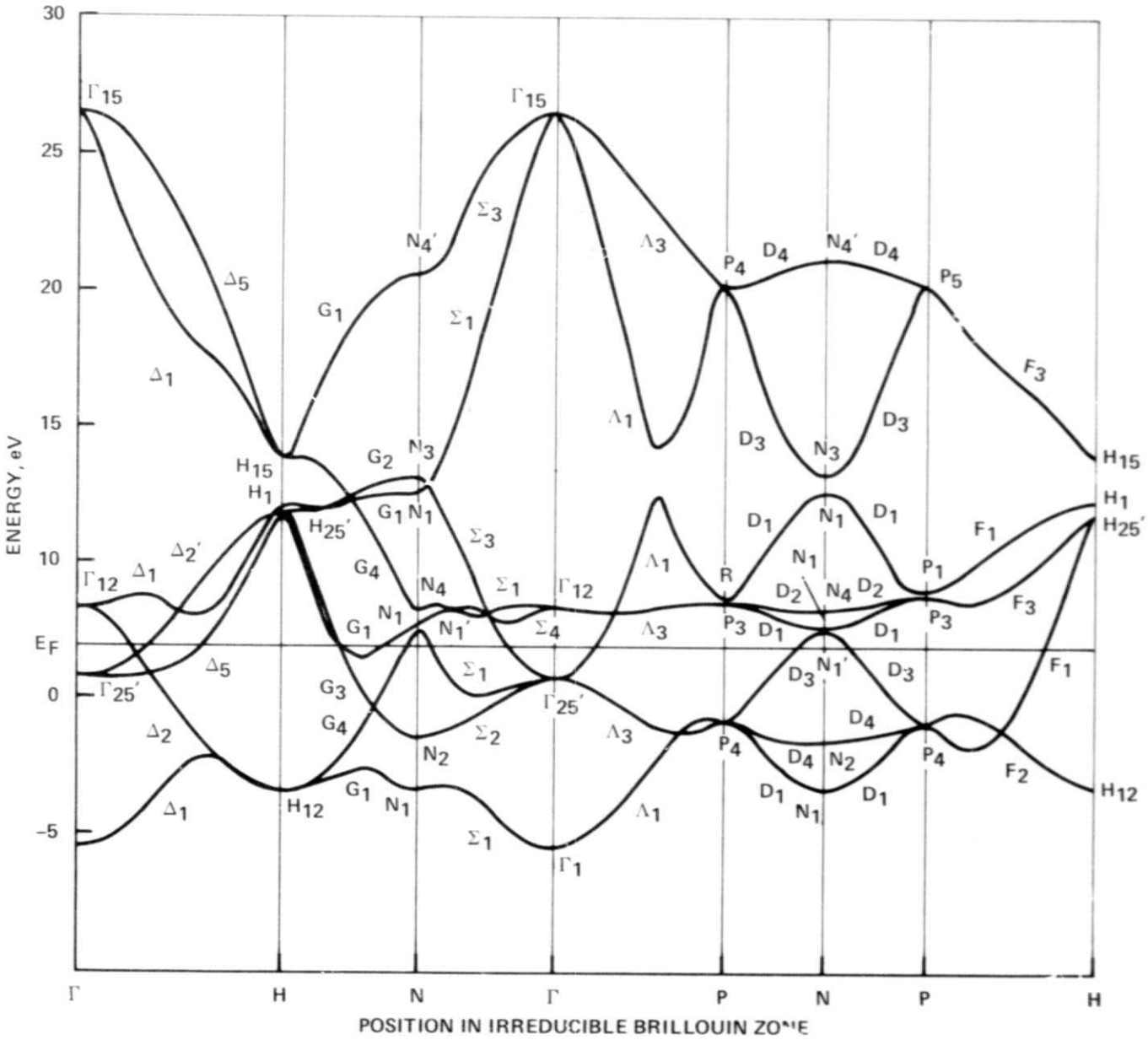


(b) Mo

Figure 1.- Concluded.

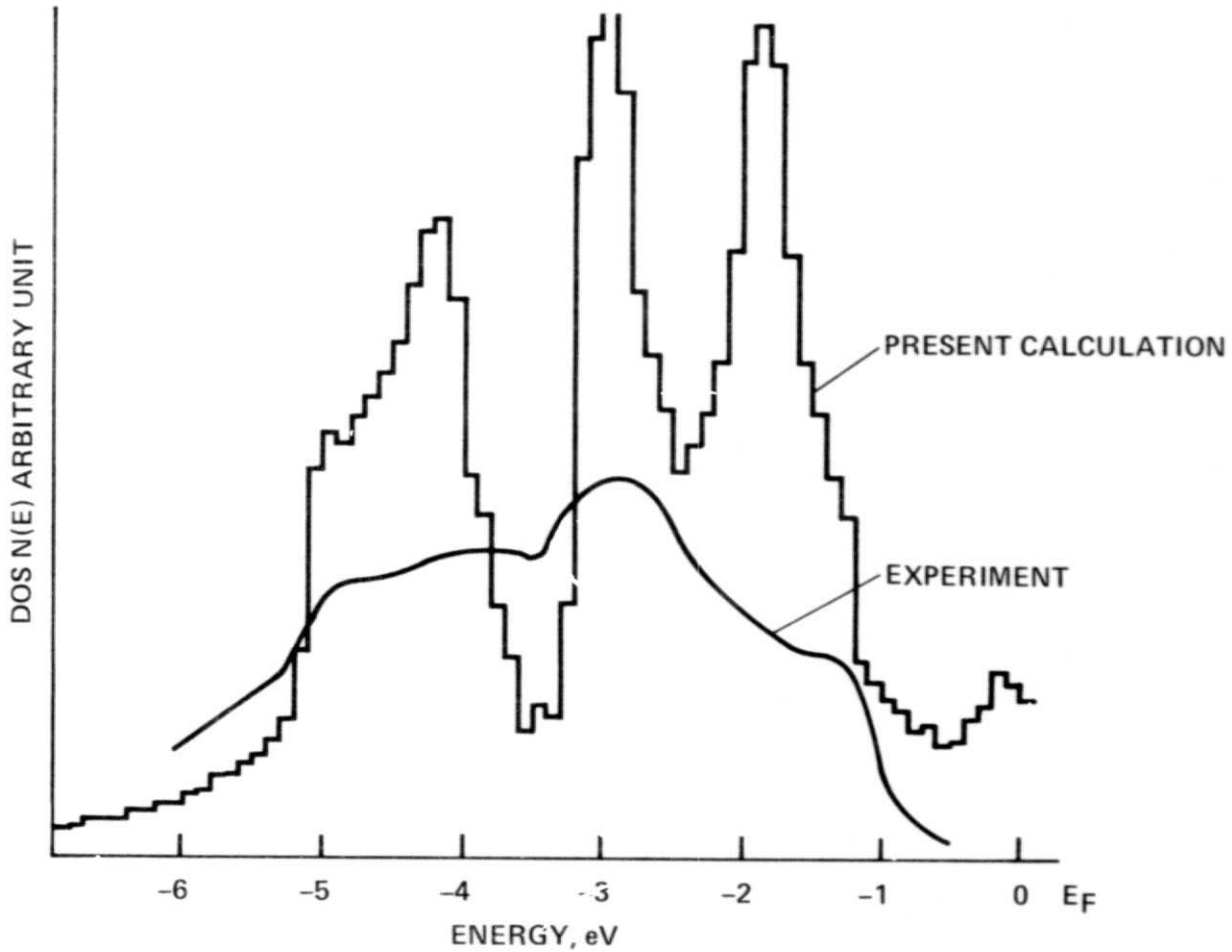


(a) W

Figure 2.- Density of states histogram.

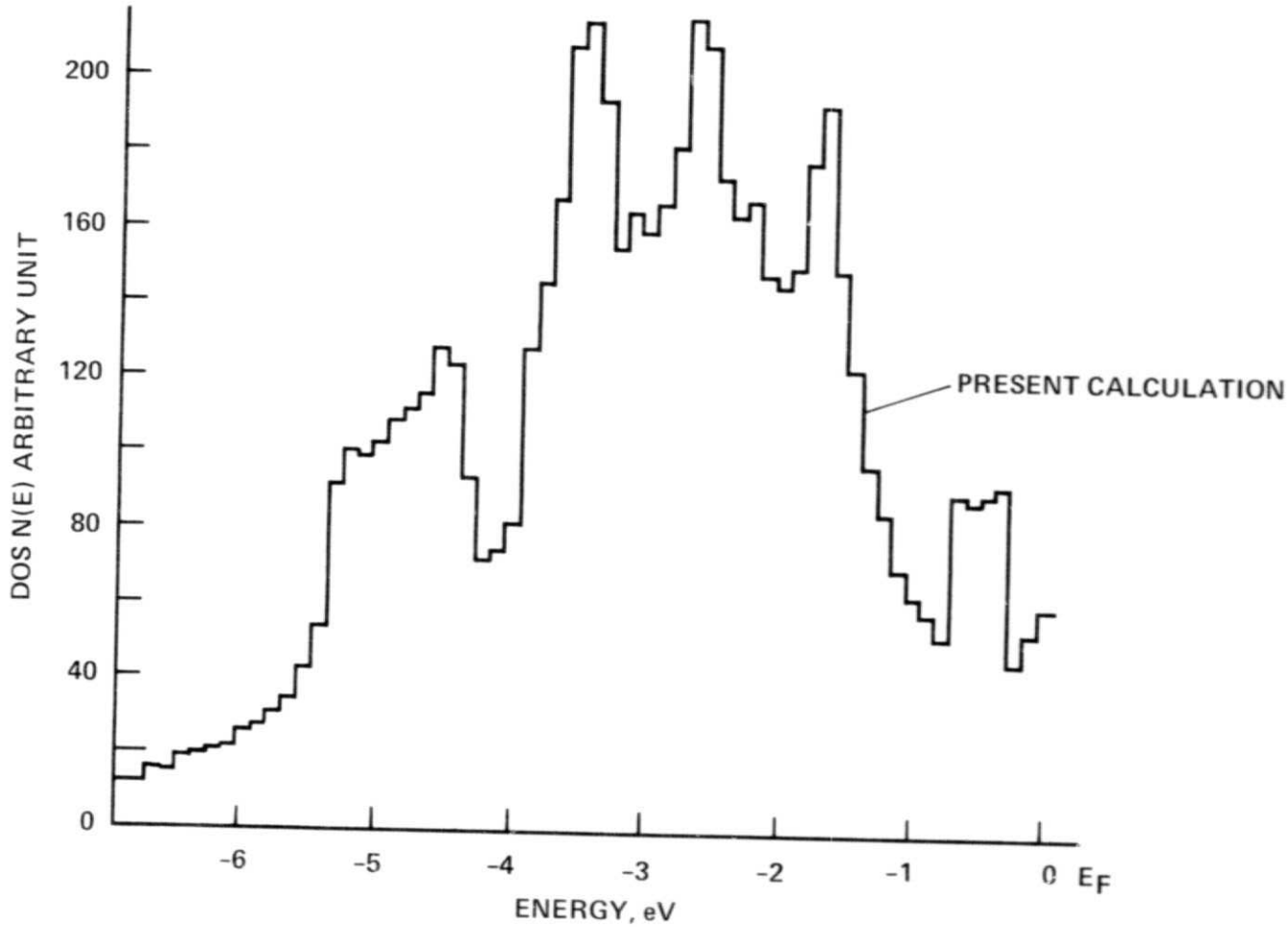


(b) Mo

Figure 2.- Concluded.

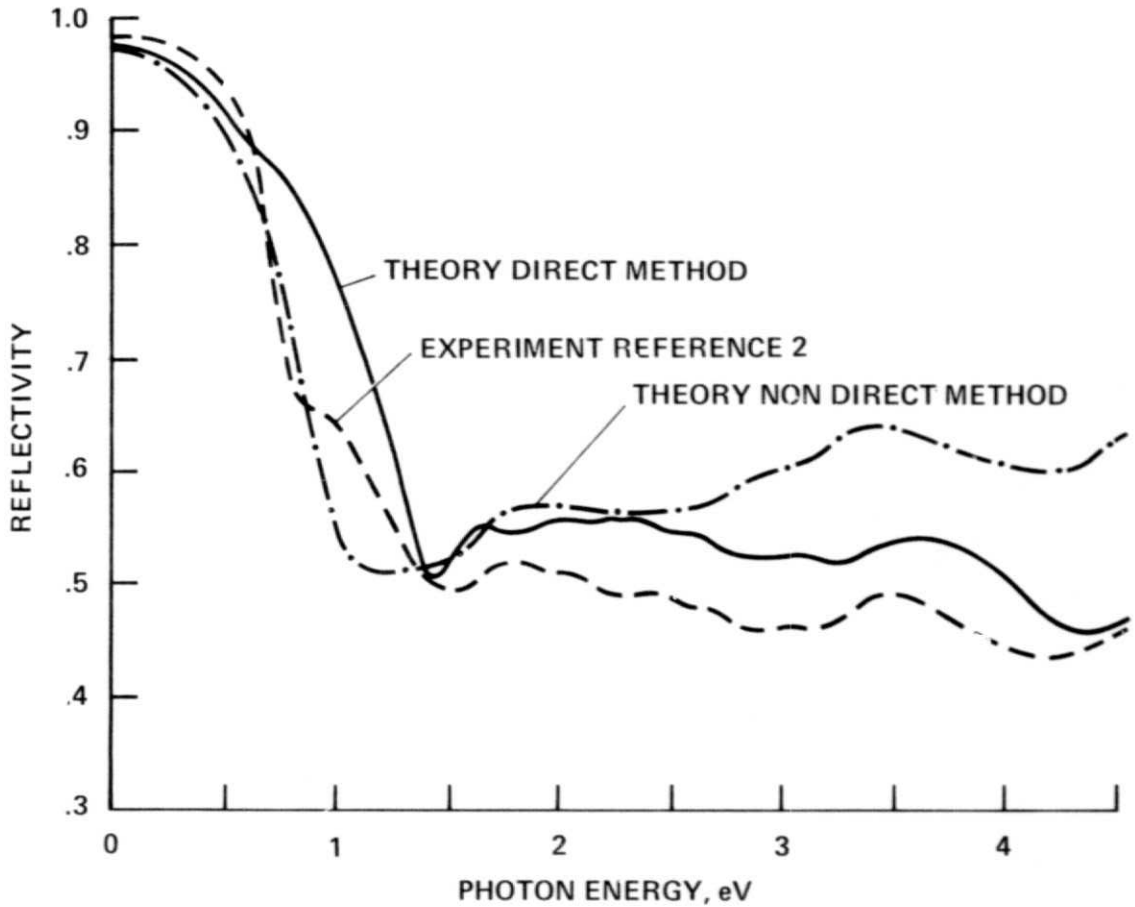


Figure 3.- Reflectivity spectrum of W.

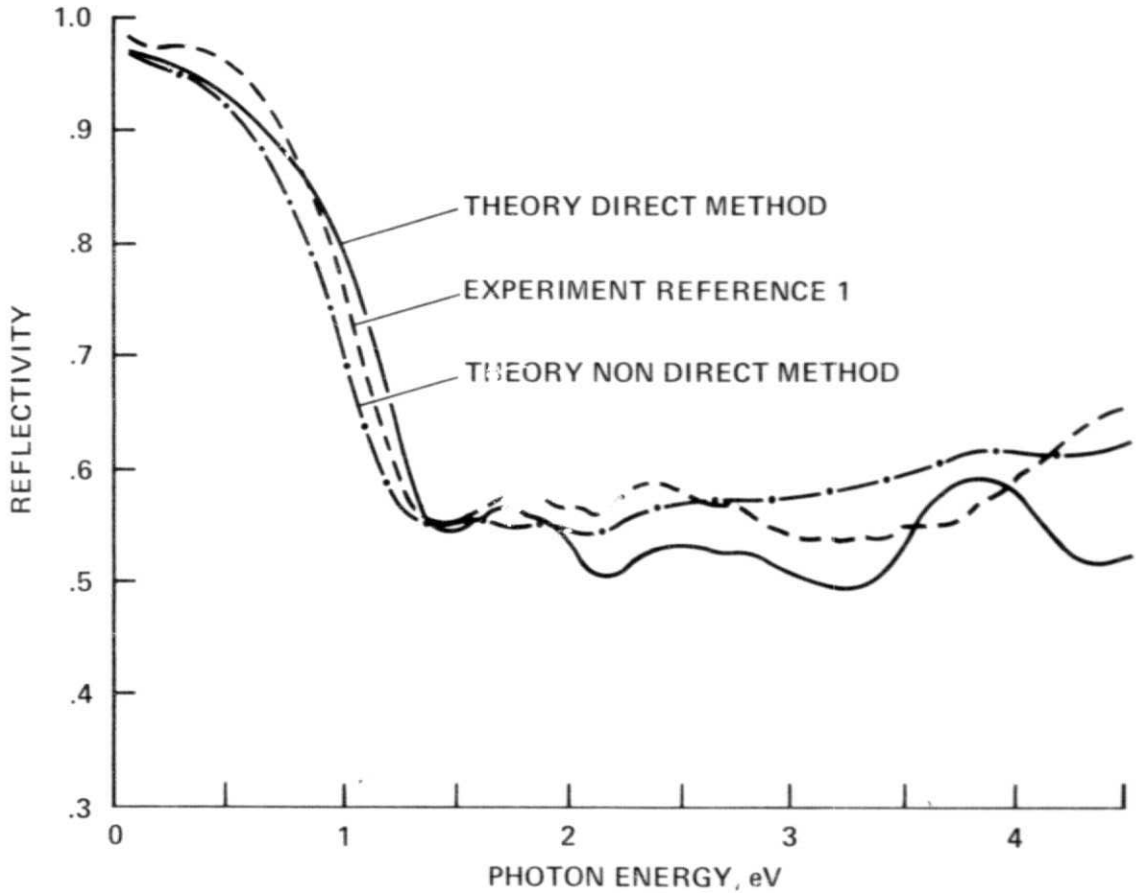


Figure 4.- Reflectivity spectrum of Mo.

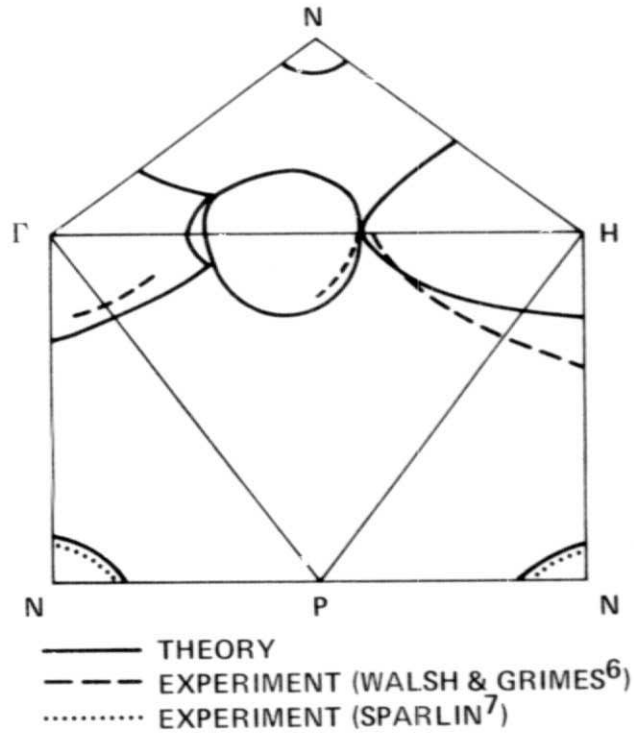


Figure 5.- Central portion of Fermi surface of W.

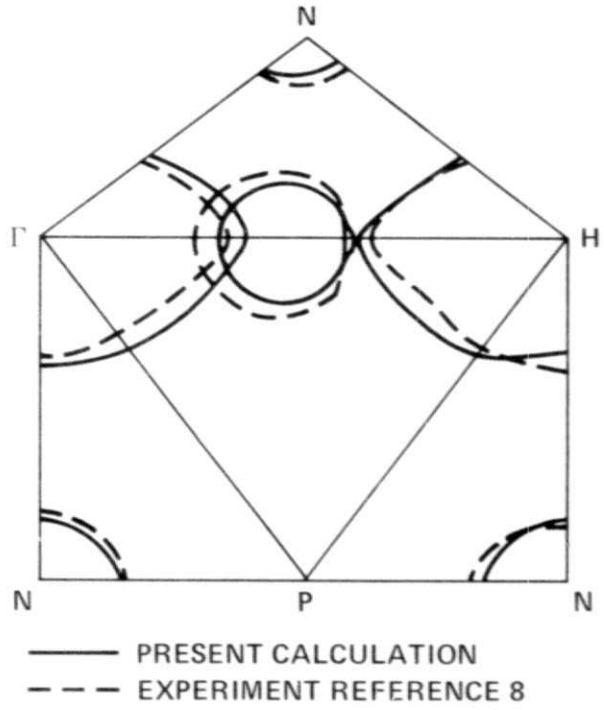


Figure 6.- Central portion of Fermi surface of Mo.

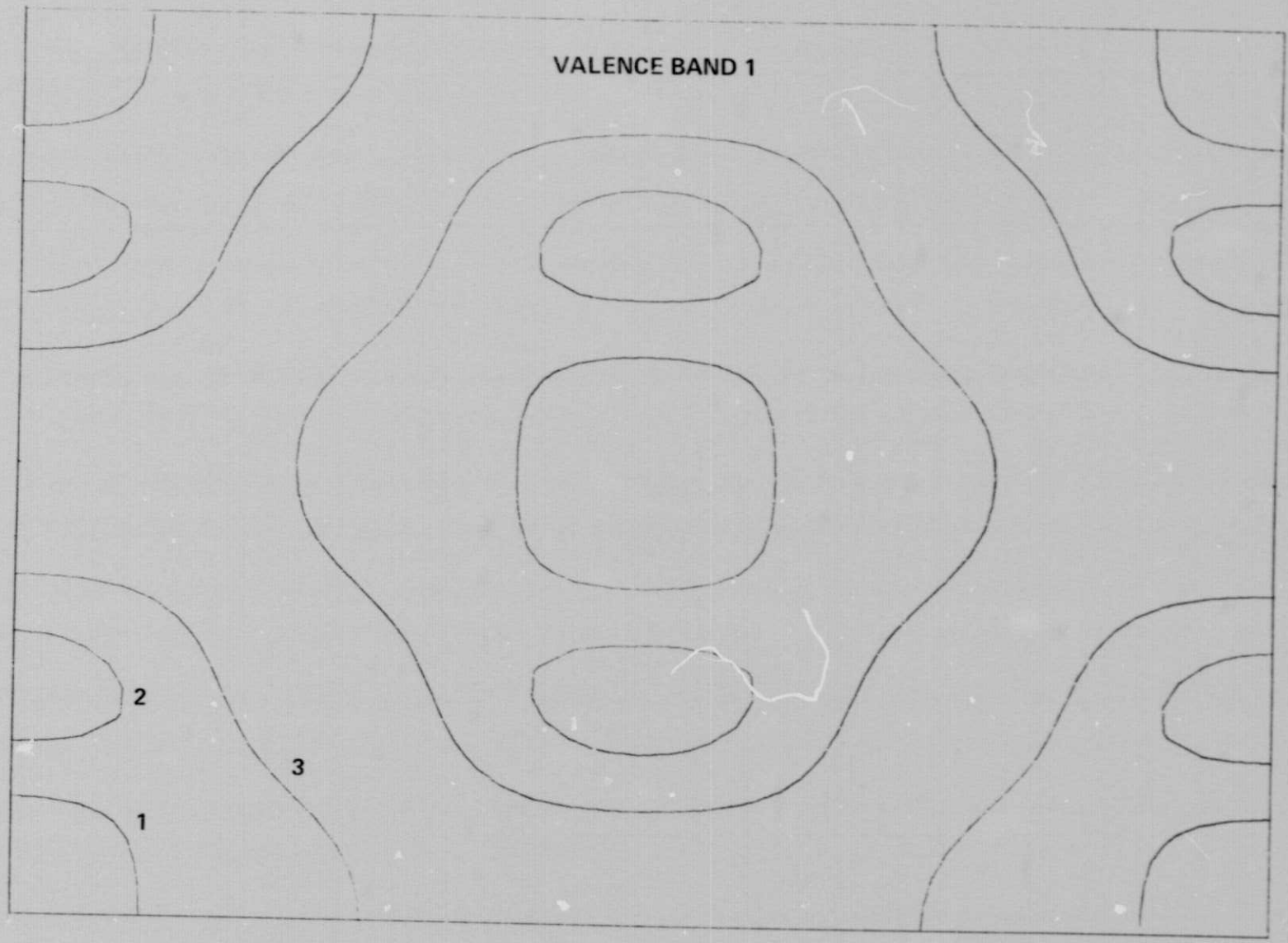


(a) W

Figure 7.- Charge distribution of valence band 1.

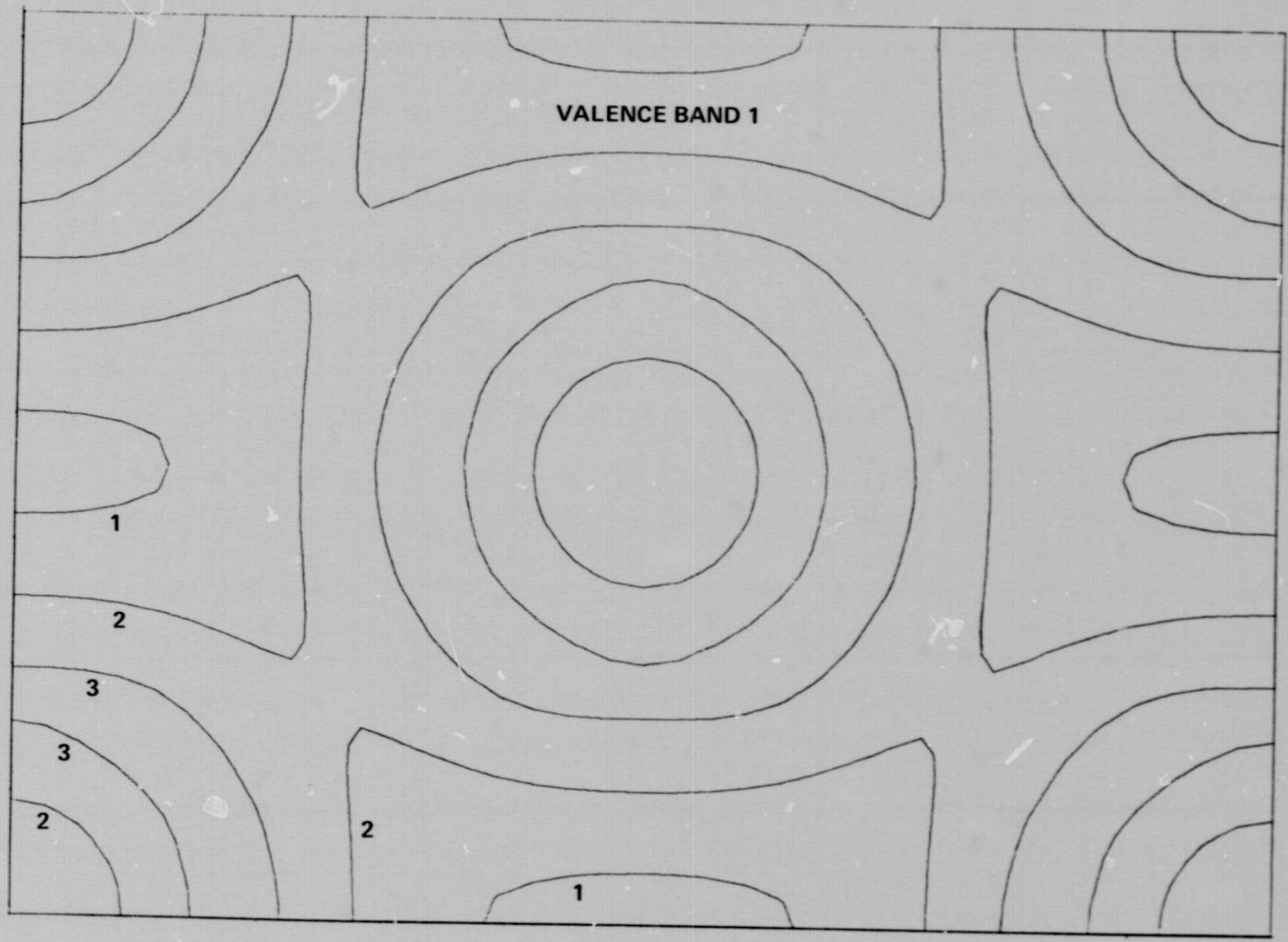


(b) Mo

Figure 7.- Concluded.

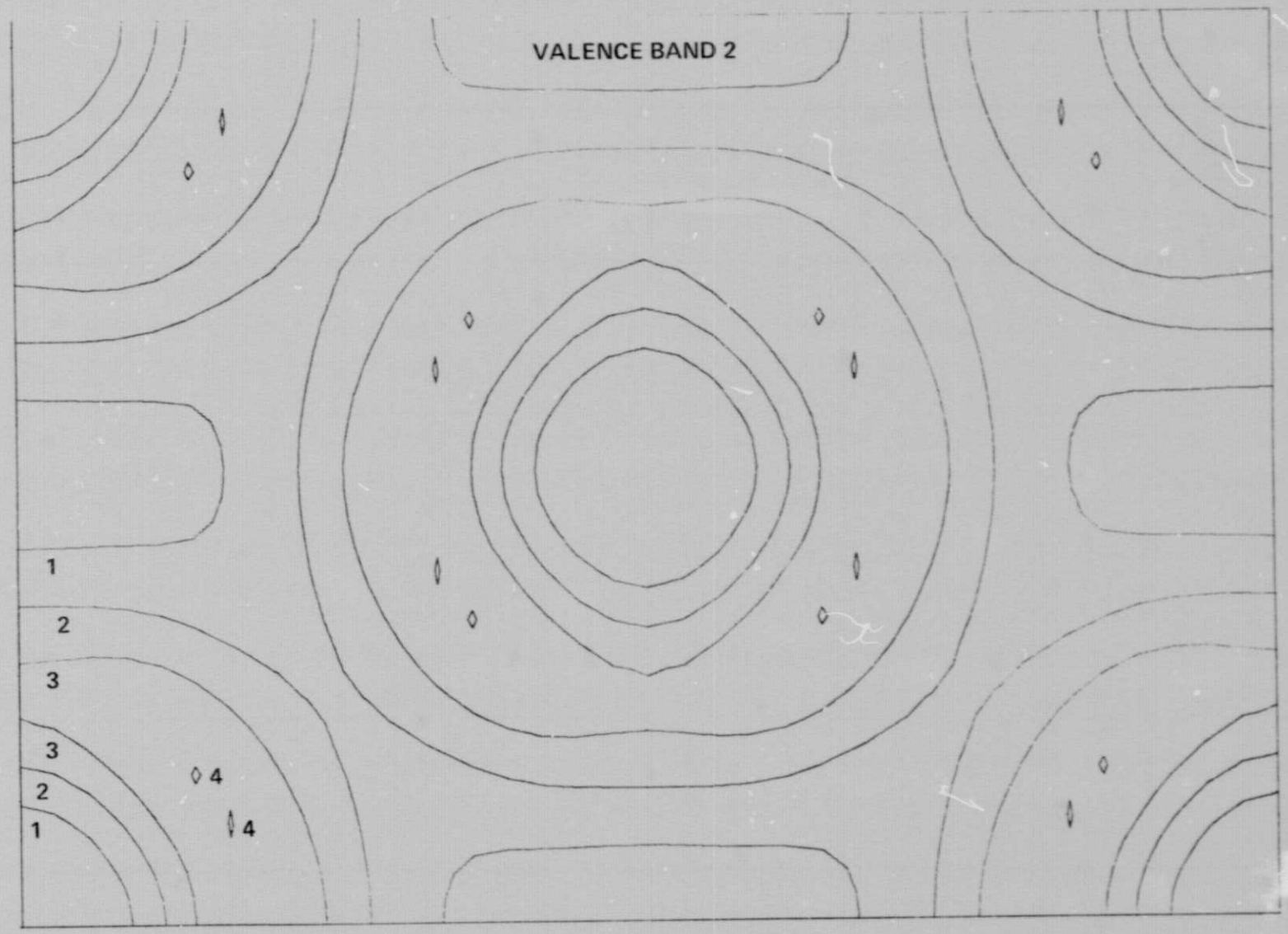


(a) W

Figure 8.- Charge distribution of valance band 2.

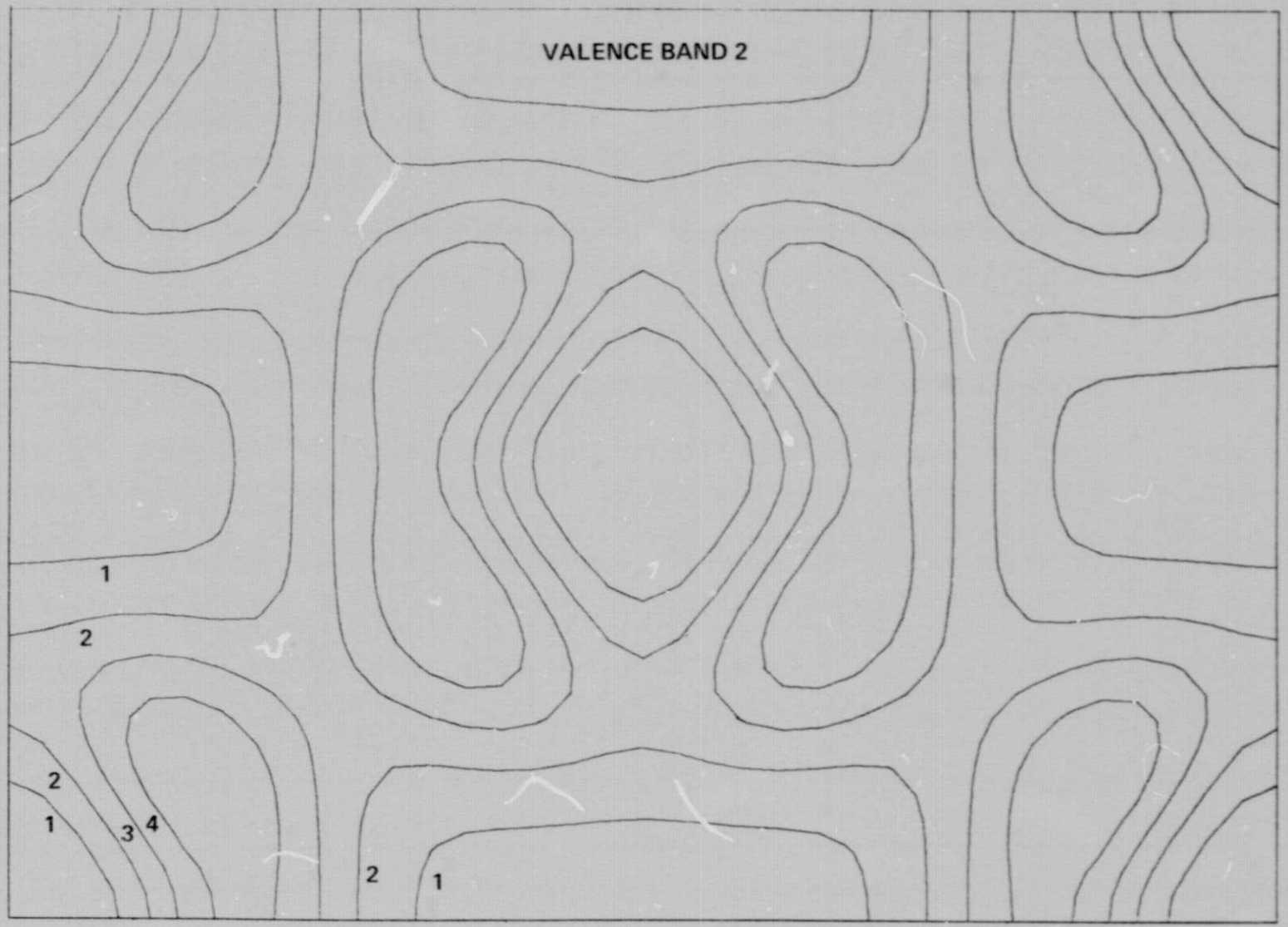


(b) Mo

Figure 8.- Concluded.

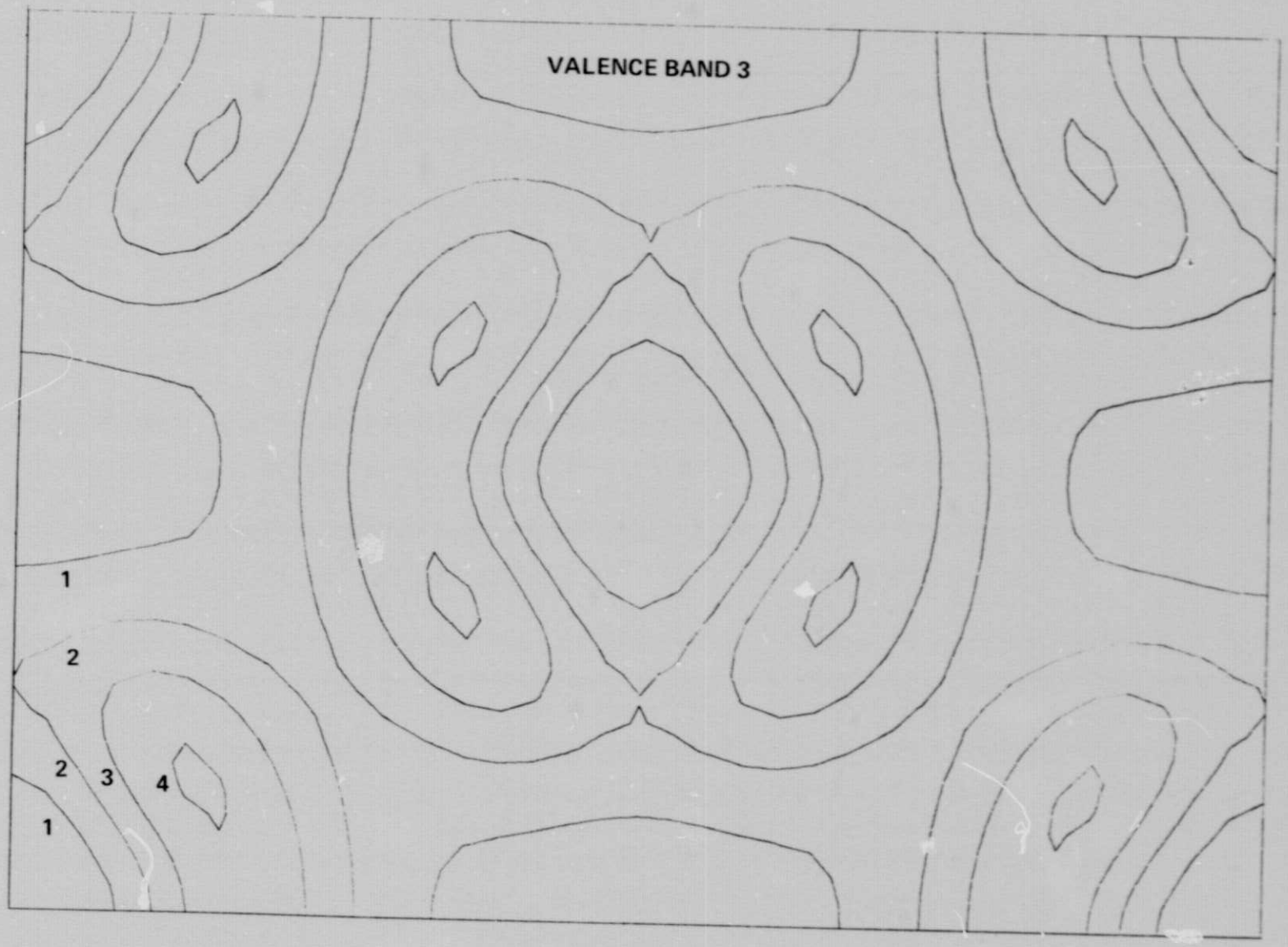


(a) W

Figure 9.- Charge distribution of valence band 3.

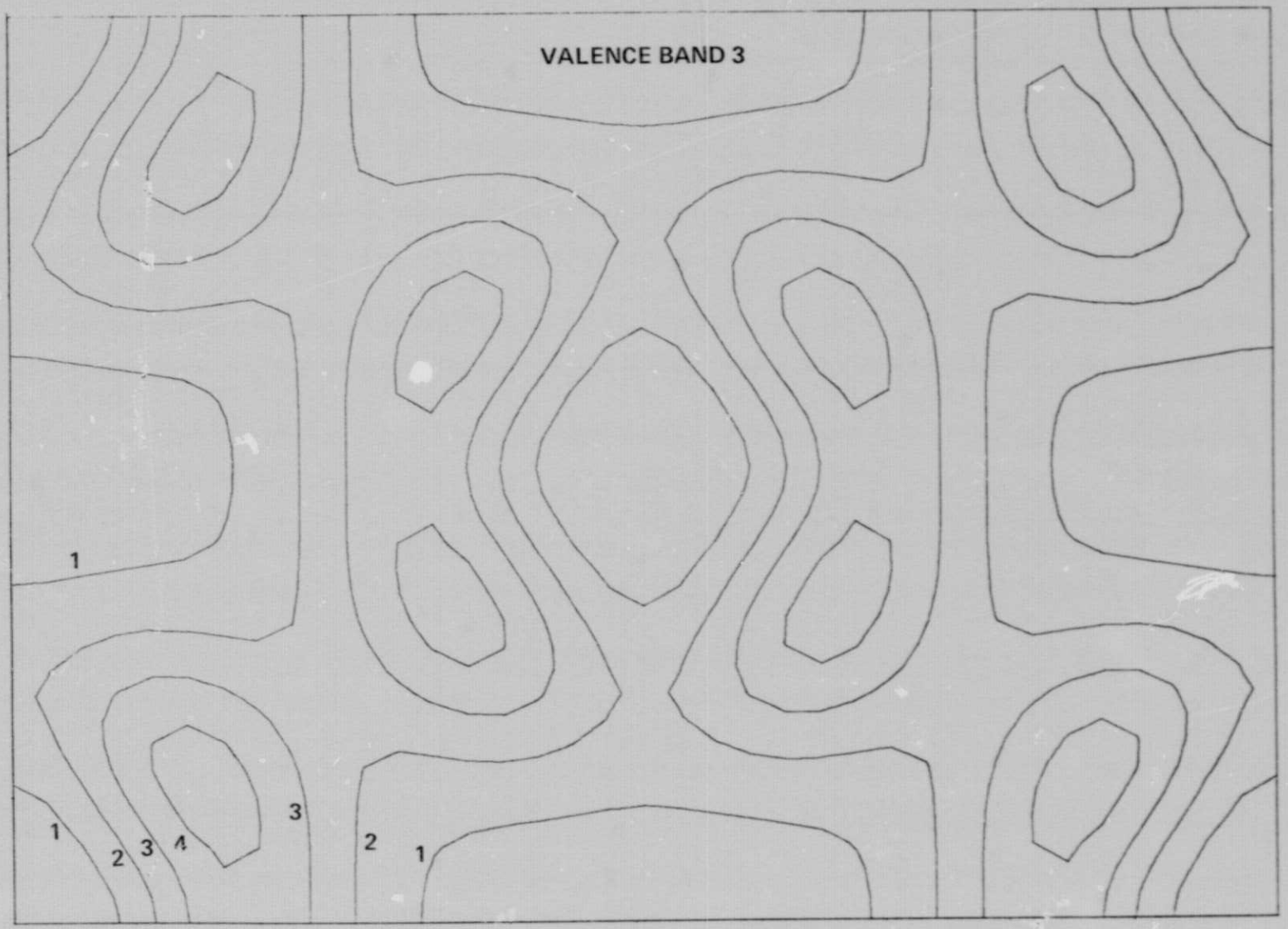


(b) Mo

Figure 9.- Concluded.

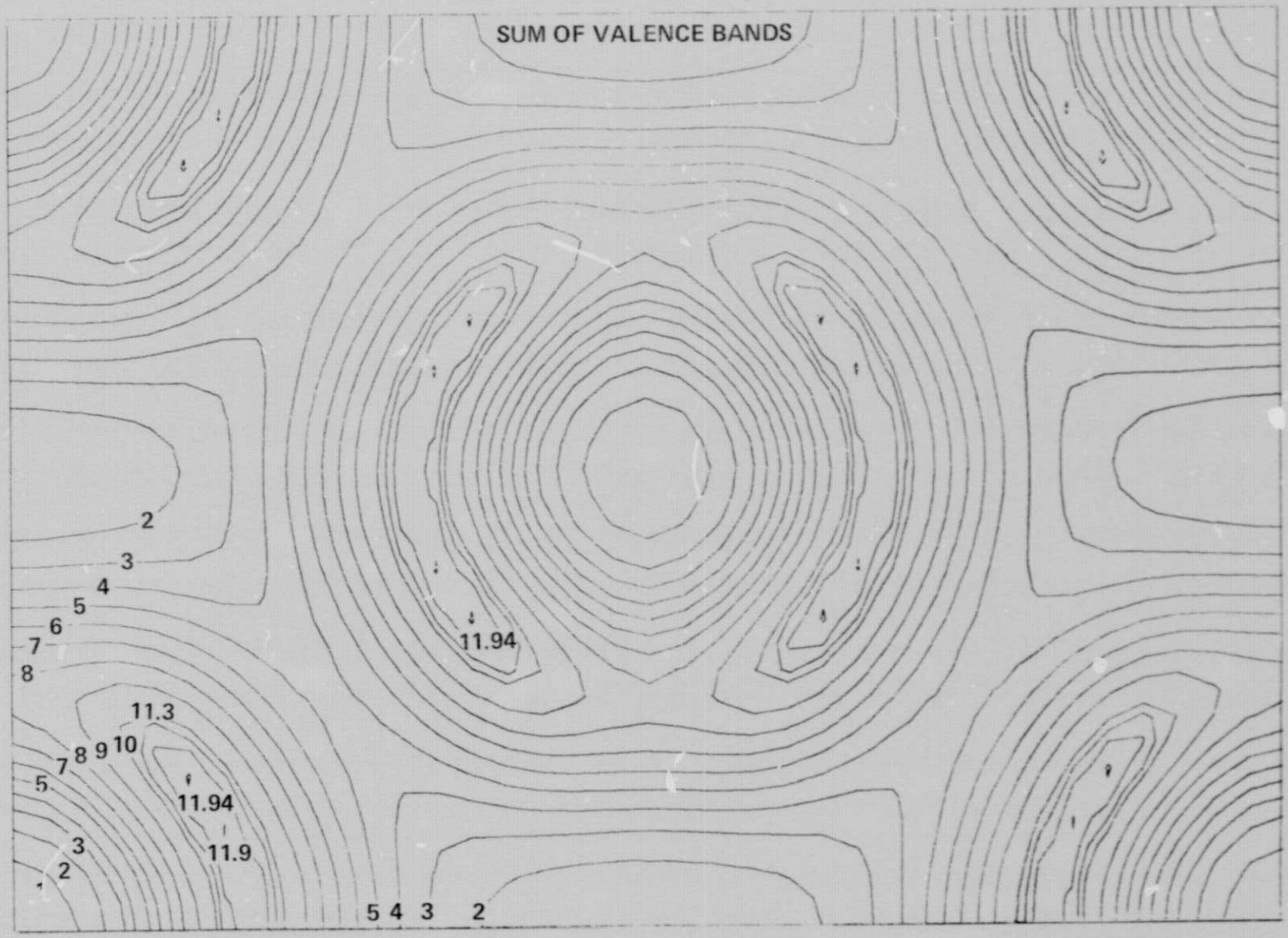


(a) W

Figure 10.- Charge distribution of occupied states (sum of valence bands).

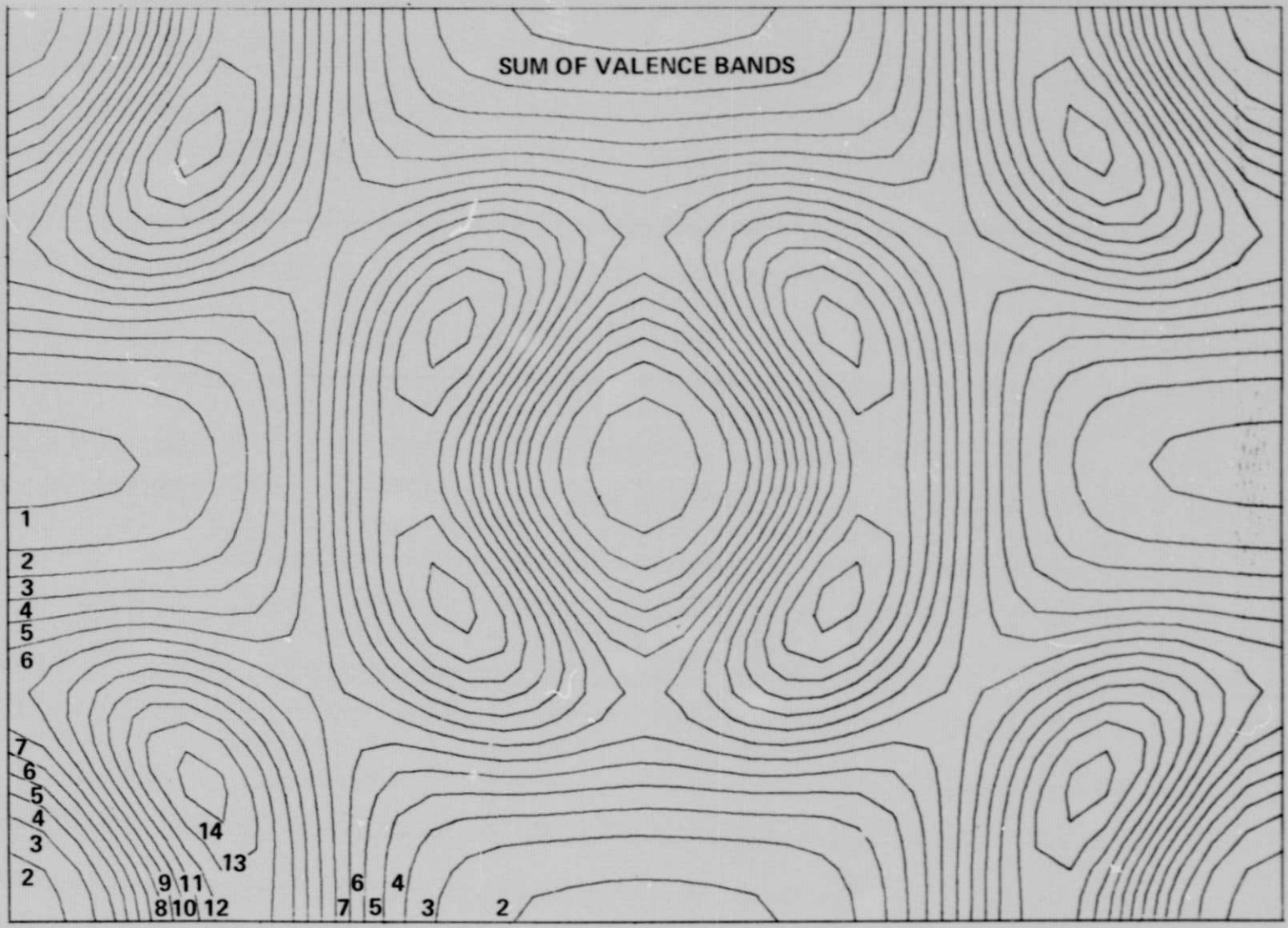


(b) Mo

Figure 10.- Concluded.